The 2009 IEEE/RSJ International Conference on
Intelligent Robots and Systems
October 11-15, 2009 St. Louis, USA

Active Vibration Control Based on a 3-DOF Dual Compliant Parallel Robot Using LQR Algorithm

Yuan Yun and Yangmin Li

Abstract— **In recent years, many applications in precision engineering require a careful isolation of the instrument from the vibration sources by adopting active vibration isolation system to achieve a very low remaining vibration level especially for the very low frequency under 10Hz vibration signals. In this paper, based on the previous research experiences in the systematical modeling and study of parallel robots, a hybrid robot is described and the vibration model is given by using Lagrange's Equations. Then the present study addresses the issues related to the active vibration control schemes for the MIMO system using LQR algorithm. Finally, numerical simulations on the effect of active vibration control are presented.**

I. INTRODUCTION

There are three fundamental control strategies to regulate or control the response of a system: passive control, semi-active control, and active control. Design and implementations of passive isolation systems have been studied for many years. Passive isolation systems generally consist of one or several stages of mass-spring-damper systems introduced in the propagation path, whose parameters are adjusted to achieve the desired corner frequency and a reasonable compromise between the amplification at resonance and the high-frequency attenuation. The passive damping is necessary to limit the amplification at resonance, but it tends to reduce the high-frequency attenuation of the isolation system. Semi-active control has been developed as a compromise between passive and active control. A semi-active control system can achieve favorable results through selective energy dissipation, but is incapable of injecting energy into a system. Active isolation has been introduced to allow to achieve simultaneously a low amplification at resonance and a large attenuation at high-frequency. Active control can change the properties of the system based on the change in the instantaneous operating conditions as measured by sensors. To counteract the vibration on precision instruments, active isolation systems are best suited, since these units achieve a very low remaining vibration level, especially for low frequency disturbances without the resonance behavior of a passive isolation system.

Active vibration control technology consists of a mixture of mechanical engineering, structural mechanics, control engineering, material sciences and computer science. Nowadays, a careful isolation of the instrument from the vibration sources is required in many precision engineering applications, which is realized by adopting active vibration isolation system to achieve a very low remaining vibration level especially for the very low frequency under 10Hz vibrations.

Active vibration isolation project based on parallel manipulator is on-going aiming to cross the bridge between the structural dynamics and control communities, while providing an overview of the potential of smart materials for sensing and actuating purposes in active vibration control. Parallel manipulators can offer the advantages of high stiffness, low inertia, and high speed capability which have been intensively researched and evaluated by industry and institutions in recent years. And some designers adopt the flexure hinges instead of conventional mechanism joints since the backlash and friction in the conventional joints influence the performances of parallel mechanisms remarkably. Micro/nano positioning manipulators and active vibration control devices are increasingly being made of parallel manipulators due to their characteristics of high precision and high speed capability.

Therefore, a lot of designers focus their attentions on multi-degree of freedom hybrid manipulators or developing wide range flexure hinges. A spatial compliant 3-DOF parallel robot with SMA pseudo-elastic flexure hinges was presented in [1], which has a workspace larger than $200 \times 200 \times 60\ mm^3$ and resolution is better than $1\mu m$. A parallel structure for macro-micro systems was proposed in [2]. In this new design, the macro-motion (DC motor) and micro motion are connected by a parallel structure, the two motions are coupled under one compliant mechanism framework. At the same time, a kind of dual parallel mechanism was developed [3], called a 6-PSS parallel mechanism and a 6-SPS one, which is integrated with wide-range flexure hinges as passive joints to ensure the large workspace of the whole system and high precision motion. A XYZ-flexure parallel mechanism was proposed with large displacement and decoupled kinematics structure [4], which has a large motion range beyond of $1mm$.

The piezo actuator is a well-known commercially available device for managing small displacements, which has the advantages of high precision, large force generation, sub-millisecond response, no magnetic fields et al. Nowadays, piezo actuators in high precision positioning systems and active vibration control systems have been investigated widely. However there are limited research works on using piezo actuators in parallel manipulator for active vibration control.

This research is concerned with the development of a

This work is supported by the Macao Science and Technology Development Fund under Grant No.:016/2008/A1 and research committee of University of Macau under Grant No.: UL016/08-Y2/EME/LYM01/FST.

Yuan Yun and Yangmin Li(corresponding author) are with the Department of Electromechanical Engineering, Faculty of Science and Technology, University of Macau, Av. Padre Toms Pereira, Taipa, Macau SAR, China, ya77406@umac.mo, ymli@umac.mo

system that can achieve three high accurate translational positioning and a 3-DOF active vibration isolation, which attenuates the vibration transmission above some corner frequencies, to protect the payload from the jitters induced by the various disturbance sources. In this paper, based on the previous research experiences in the systematical modeling and study of parallel robots, a novel dual 3-DOF parallel robot with flexure hinges will be described. A vibration model of the parallel manipulator will be presented by Lagrangian's equations. Then the present study addresses the issues related to the active vibration control schemes for the MIMO system using LQR algorithm with the piezo actuators as the actuators, laser sensors for displacement and accelerometers as the sensors. Finally, numerical simulations about the dynamic characteristics and control effects will be presented.

II. SYSTEM DESCRIPTION

The designed 3-DOF dual parallel platform is a 3-DOF dual parallel mechanism combining a 3-PUU parallel mechanism with another spatial 3-UPU one. In the 3-PUU parallel structure, the prismatic actuators provide three translational macro motions with micron level accuracy and cubic centimeter workspace. At the same time, the micro motion is provided by a spatial 3-UPU structure which can increase the accuracy of the whole system to the nanometer level or provide a strictly acceleration level for payload placed on the moving platform. 3-PUU and 3-UPU kinematical structures with conventional mechanical joints can be arranged to achieve only translational motions with some certain geometric conditions satisfied.

Using flexure hinges at all joints, the parallel platform consists of a mobile platform, a fixed base, and three limbs with identical kinematic structure. Each limb connects the mobile platform to the fixed base by one prismatic actuator, one flexure universal (U) hinge and a piezo actuator followed by another U joint in sequence as shown in Fig. 1, where the first U joint is fixed at the prismatic actuator and the second one connects to the moving platform actuated by a piezo actuator to offer the micro motions with merits of involving smooth motion, high accuracy, and fast response, etc. The flexure universal hinge is a slender shaft configuration with very high torsional stiffness which is adopted as passive joint to ensure the large workspace of the whole system and high precision motion. High precision ceramic motors are adopted as the prismatic actuators to provide the macro motion for the mechanism.

III. DYNAMIC MODEL

Since the macro motion is adopted for the rough positioning, the kinematic analysis is necessary for the 3-PUU structure. The details have been published in [5]. In this section, the vibration model using Lagrange's equations will be described first for the 3-UPU structure, and then Kane's dynamics modeling will be built up to verify the results.

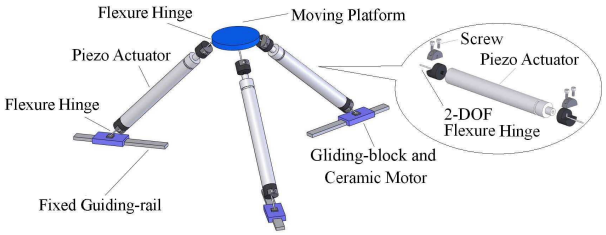

Fig. 1. The 3-DOF 3-PUU/3-UPU dual parallel manipulator.

A. Kinematic Analysis

In this case, the prismatic actuators for macro motion are self-locked when the micro motion is available.

1) Coordinate System: Let $\mathbf{L}=[l_1\ l_2\ l_3]^T$ be the vector of the three PZT actuated length variables and the vector $\mathbf{r}_{oo'}=[x\ y\ z]^T$ of the reference point o' be the position of the moving platform. As shown in Fig. 2, let $\mathbf{b}_i$ be the vector $\overrightarrow{oB_i}$ and $\mathbf{m}_i$ be the vector $\overrightarrow{o'M_i}$. The mass of moving platform is M. The mass of each strut is m_l. C_i^* (i=1, $\cdots$, 3) is the center of mass for the ith limb. Let a limb fixed right-handed coordinate system with origin C_i^* (i=1, $\cdots$, 3) located at the center of mass for the ith limb, with axis directions determined by an orthonormal set of unit vectors $\widehat{\mathbf{c}}_j^i$ (j=1,$\cdots$,3). The hat indicates unit length, the index i corresponds to the ith limb, and the index j distinguishes the three vectors. $\widehat{\mathbf{c}}_3^i$ is along the ith limb, toward the ith flexure hinge which connects the moving platform. $\widehat{\mathbf{c}}_2^i$ is perpendicular to the vector $\overrightarrow{oB_i}$ when the moving platform is in its home position, and $\widehat{\mathbf{c}}_1^i$ is in the direction $\widehat{\mathbf{c}}_2^i \times \widehat{\mathbf{c}}_3^i$. Let a reference frame $\widehat{\mathbf{s}}_j$ attach to the fixed platform at the center o with the $\widehat{\mathbf{s}}_1$ toward the point B_1 and $\widehat{\mathbf{s}}_3$ vertical the fixed platform. Fix a coordinate system $\widehat{\mathbf{f}}_j$ to the moving platform at the center o' with $\widehat{\mathbf{f}}_1$ toward the point M_i and $\widehat{\mathbf{f}}_3$ vertical the moving platform. $\Re$ is a three-order identity transformation matrix from $\widehat{\mathbf{f}}_j$ coordinate system to $\widehat{\mathbf{s}}_j$. $\Re_{ci}$ is the transformation matrix from $\widehat{\mathbf{c}}_j$ coordinate system to $\widehat{\mathbf{s}}_j$.

In order to determine the angles of flexure hinges directly, an initial coordinate system is set on origin C_i^* with axis directions determined by an orthonormal set of unit vectors $\widehat{\mathbf{c}}_{j0}^i$ when the moving platform is in the home position. The axis directions are located coincident with the corresponding limb fixed coordinate system $\widehat{\mathbf{c}}_j^i$ when the moving platform is in the initial position. Let the orientation of the $\widehat{\mathbf{c}}_j^i$ coordinate system, relative to the $\widehat{\mathbf{c}}_{j0}^i$, be described by consecutive positive rotations q_1^i about the $\widehat{\mathbf{c}}_{10}^i$ and q_2^i about the moved two-axis. The rotation matrix $\Re_{ci0}$ is:

$$\Re_{ci0} = \begin{bmatrix} \widehat{\mathbf{c}}_{10}^i & \widehat{\mathbf{c}}_{20}^i & \widehat{\mathbf{c}}_{30}^i \end{bmatrix}^{-1} \begin{bmatrix} \widehat{\mathbf{c}}_1^i & \widehat{\mathbf{c}}_2^i & \widehat{\mathbf{c}}_3^i \end{bmatrix}. \quad (1)$$

It is assumed that the small-angle approximations hold for angles q_k^i, the rotation matrix is:

$$\Re_{ci0} = \begin{bmatrix} 1 & 0 & q_2^i \\ 0 & 1 & -q_1^i \\ -q_2^i & q_1^i & 1 \end{bmatrix}. \quad (2)$$

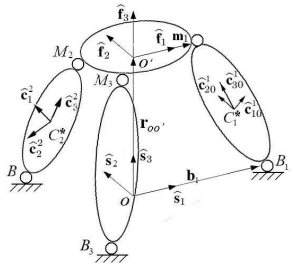

Fig. 2. Coordinate system of the 3-UPU parallel platform

2) Generalized Speeds for the System: Define generalized speeds **u** for the system as the time rate of change of the generalized coordinates of **q**=$[x\ y\ z]^T$ in the inertial reference frame:

$$\mathbf{u} = \begin{bmatrix} \dot{x} & \dot{y} & \dot{z} \end{bmatrix}^T. \tag{3}$$

An intermediate reference frame is introduced previously to permit describing the angular velocity of each limb to the initial limb position. Designate the unit vectors of these intermediate reference frames by $\widehat{\mathbf{m}}_j^i$. The expressions for the angular velocities of the reference frame of each upper arm with respect to initial reference frame of upper arm are:

$$\underline{\omega}_{C_i^*} = -\dot{q}_1^i \widehat{\mathbf{c}}_{10}^i - \dot{q}_2^i \widehat{\mathbf{m}}_2^i. \tag{4}$$

The position vectors are:

$$\mathbf{r}_{oo'} = l_i \widehat{\mathbf{c}}_3^i + \mathbf{b}_i - \mathbf{m}_i,$$

$$\mathbf{r}_{m_i} = l_i \widehat{\mathbf{c}}_3^i + \mathbf{b}_i,\ \mathbf{r}_{C_i^*} = \frac{l_i}{2} \widehat{\mathbf{c}}_3^i + \mathbf{b}_i. \tag{5}$$

Differentiating Eq. (5) with respect to time:

$$\mathbf{v}_{o'} = \dot{l}_i \widehat{\mathbf{c}}_3^i + l_i \underline{\omega}_{C_i^*} \times \widehat{\mathbf{c}}_3^i \tag{6}$$

$$\mathbf{v}_{m_i} = \mathbf{v}_{o'},\ \mathbf{v}_{C_i^*} = \frac{\dot{l}_i \widehat{\mathbf{c}}_3^i + l_i \underline{\omega}_{C_i^*} \times \widehat{\mathbf{c}}_3^i}{2} = \frac{\mathbf{v}_{o'}}{2}.$$

Dot-multiplying both sides of Eq. (6) by $\widehat{\mathbf{c}}_3^i$:

$$(\widehat{\mathbf{c}}_3^i)^T \mathbf{v}_{o'} = \dot{l}_i \ (i = 1, 2, 3) \tag{7}$$

which can be assembled into a matrix form:

$$\begin{bmatrix} \dot{l}_1 & \dot{l}_2 & \dot{l}_3 \end{bmatrix}^T = \mathbf{A} \cdot \mathbf{v}_{o'} \tag{8}$$

where $\mathbf{A} = \begin{bmatrix} (\widehat{\mathbf{c}}_3^1) & (\widehat{\mathbf{c}}_3^2) & (\widehat{\mathbf{c}}_3^3) \end{bmatrix}^T$.

Cross-multiplying both sides of Eq. (6) by $\widehat{\mathbf{c}}_3^i$:

$$\underline{\omega}_{C_i^*} = \frac{\widehat{\mathbf{c}}_3^i \times \mathbf{v}_{o'}}{l_i} \tag{9}$$

The linearized accelerations are:

$$\mathbf{a}_{o'} = (2\dot{l}_i \underline{\omega}_{C_i^*} + l_i \underline{\varepsilon}_{C_i^*}) \times \widehat{\mathbf{c}}_3^i + l_i \underline{\omega}_{C_i^*} \times (\underline{\omega}_{C_i^*} \times \widehat{\mathbf{c}}_3^i) + \ddot{l}_i \widehat{\mathbf{c}}_3^i$$

$$\mathbf{a}_{C_i^*} = \frac{\mathbf{a}_{o'}}{2} \tag{10}$$

Cross-multiplying both sides of Eq. (10) by $\widehat{\mathbf{c}}_3^i$, the angular acceleration of each limb can be obtained by:

$$\underline{\varepsilon}_{C_i^*} = \frac{\widehat{\mathbf{c}}_3^i \times \mathbf{a}_{o'} - 2\dot{l}_i \underline{\omega}_{C_i^*} - l_i (\underline{\omega}_{C_i^*} \cdot \widehat{\mathbf{c}}_3^i)(\underline{\omega}_{C_i^*} \times \widehat{\mathbf{c}}_3^i)}{l_i} \tag{11}$$

B. Vibration Model

In this paper, the vibrational model is established by using Lagrange's equation which is a well known tool for establishing equations of motion of discrete systems. The key point of Lagrange's equations is kinetic energy, which can be formulated favorably with respect to a moving coordinate system as well.

1) Kinetic Energy of the System: For the moving platform, the kinetic energy can be given by

$$E_{kM} = \frac{1}{2} M (\dot{x}^2 + \dot{y}^2 + \dot{z}^2) \tag{12}$$

For each limb, assume rotations about a fixed axis, the kinetic energy can be given by

$$E_{kl_i} = \frac{1}{2} m_l \|\mathbf{v}_{C_i^*}\|^2 + \frac{1}{2} I_{C_i} \underline{\omega}_{C_i^*}^2 \tag{13}$$

where

$$I_{C_i} = \frac{1}{3} m_l l_i^2$$

and according to Eq. (4), the kinetic energy of the whole system can be derived by

$$E_k = E_{kM} + \sum_{i=1}^{3} E_{kl_i} = \frac{1}{2} M (\dot{x}^2 + \dot{y}^2 + \dot{z}^2) + \sum_{i=1}^{3} \Big(\frac{1}{2} m_l \|\mathbf{v}_{C_i^*}\|^2$$

$$+ \frac{1}{2} I_{C_i} ((\dot{q}_1^i)^2 + (\dot{q}_2^i)^2) \Big) = \Big(\frac{1}{2} M + \frac{3}{8} m_l \Big) (\dot{x}^2 + \dot{y}^2 + \dot{z}^2)$$

$$+ \sum_{i=1}^{3} \frac{1}{6} m_l l_i^2 ((\dot{q}_1^i)^2 + (\dot{q}_2^i)^2) \Big) \tag{14}$$

2) Potential Energy of the System: The potential energy of moving platform is given by

$$E_{pM} = Mgz. \tag{15}$$

Since the system is investigated in tiny vibration environment, according to the Eq. (5), we can obtain

$$\widehat{\mathbf{c}}_3^i = \frac{1}{l_i} \begin{bmatrix} x - x_{b_i} + x_{m_i} \\ y - y_{b_i} + y_{m_i} \\ z - z_{b_i} + z_{m_i} \end{bmatrix} \tag{16}$$

Let

$$\begin{bmatrix} \widehat{\mathbf{c}}_{10}^i & \widehat{\mathbf{c}}_{20}^i & \widehat{\mathbf{c}}_{30}^i \end{bmatrix}^{-1} = \begin{bmatrix} r_{11}^i & r_{12}^i & r_{13}^i \\ r_{21}^i & r_{22}^i & r_{23}^i \\ r_{31}^i & r_{32}^i & r_{33}^i \end{bmatrix} \tag{17}$$

According to Eq. (1) and (2), the consecutive positive rotations q_1^i and q_2^i about the moved two-axis are:

$$\frac{1}{l_i} \begin{bmatrix} r_{11}^i & r_{12}^i & r_{13}^i \\ r_{21}^i & r_{22}^i & r_{23}^i \\ r_{31}^i & r_{32}^i & r_{33}^i \end{bmatrix} \begin{bmatrix} x - x_{b_i} + x_{m_i} \\ y - y_{b_i} + y_{m_i} \\ z - z_{b_i} + z_{m_i} \end{bmatrix} = \begin{bmatrix} q_2^i \\ -q_1^i \\ 1 \end{bmatrix}$$

$$q_1^i = H_{1i} - \frac{r_{21}^i}{l_i} x - \frac{r_{22}^i}{l_i} y - \frac{r_{23}^i}{l_i} z$$

$$q_2^i = H_{2i} + \frac{r_{11}^i}{l_i} x + \frac{r_{12}^i}{l_i} y + \frac{r_{13}^i}{l_i} z \tag{18}$$

where

$$H_{1i} = \frac{r_{21}^i}{l_i}(x_{b_i} - x_{m_i}) + \frac{r_{22}^i}{l_i}(y_{b_i} - y_{m_i}) + \frac{r_{23}^i}{l_i}(z_{b_i} - z_{m_i})$$

$$H_{2i} = \frac{r_{11}^i}{l_i}(x_{m_i} - x_{b_i}) + \frac{r_{12}^i}{l_i}(y_{m_i} - y_{b_i}) + \frac{r_{13}^i}{l_i}(z_{m_i} - z_{b_i})$$

For each limb, the potential energy can be written as:

$$E_{pl_i} = m_l g \frac{z - z_{b_i} + z_{m_i}}{2} + k_1^i (q_1^i)^2 + k_2^i (q_2^i)^2 \qquad (19)$$

Hence, the potential energy of the whole system can be given by

$$E_p = Mgz + \sum_{i=1}^{3}(m_l g \frac{z - z_{b_i} + z_{m_i}}{2} + k_1^i (q_1^i)^2 + k_2^i (q_2^i)^2) \qquad (20)$$

3) Lagrange's Equations: Let F_{Dj} and $F_j^{a_i}$ be the disturbance force and the actuated force of each limb associated to the q_j respectively. The Lagrange's equations are:

$$\frac{d}{dt}(\frac{\partial E_k}{\partial u_j}) - \frac{\partial E_k}{\partial q_j} + \frac{\partial E_p}{\partial q_j} = F_{Dj} + \sum_{i=1}^{3} F_j^{a_i} \qquad (21)$$

where

$$\frac{d}{dt}(\frac{\partial E_k}{\partial \dot{x}}) = (M + \frac{3}{4}m_l)\ddot{x} + \sum_{i=1}^{3}\frac{1}{3}m_l(((r_{21}^i)^2 + (r_{11}^i)^2)\ddot{x}$$
$$+(r_{22}^i r_{21}^i + r_{12}^i r_{11}^i)\ddot{y} + (r_{23}^i r_{21}^i + r_{13}^i r_{11}^i)\ddot{z})$$

$$\frac{d}{dt}(\frac{\partial E_k}{\partial \dot{y}}) = (M + \frac{3}{4}m_l)\ddot{y} + \sum_{i=1}^{3}\frac{1}{3}m_l((r_{21}^i r_{22}^i + r_{11}^i r_{12}^i)\ddot{x}$$
$$+((r_{22}^i)^2 + (r_{12}^i)^2)\ddot{y} + (r_{23}^i r_{22}^i + r_{13}^i r_{12}^i)\ddot{z})$$

$$\frac{d}{dt}(\frac{\partial E_k}{\partial \dot{z}}) = (M + \frac{3}{4}m_l)\ddot{z} + \sum_{i=1}^{3}\frac{1}{3}m_l((r_{21}^i r_{23}^i + r_{11}^i r_{13}^i)\ddot{x}$$
$$+(r_{22}^i r_{23}^i + r_{12}^i r_{13}^i)\ddot{y} + ((r_{23}^i)^2 + (r_{13}^i)^2)\ddot{z})$$

$$\frac{\partial E_k}{\partial x} = 0, \frac{\partial E_k}{\partial y} = 0, \frac{\partial E_k}{\partial z} = 0$$

$$\frac{\partial E_p}{\partial x} = \sum_{i=1}^{3}(2k_1^i(-\frac{r_{21}^i}{l_i})(H_{1i} - \frac{r_{21}^i}{l_i}x - \frac{r_{22}^i}{l_i}y - \frac{r_{23}^i}{l_i}z)$$
$$+2k_2^i(\frac{r_{11}^i}{l_i})(H_{2i} + \frac{r_{11}^i}{l_i}x + \frac{r_{12}^i}{l_i}y + \frac{r_{13}^i}{l_i}z))$$

$$\frac{\partial E_p}{\partial y} = \sum_{i=1}^{3}(2k_1^i(-\frac{r_{22}^i}{l_i})(H_{1i} - \frac{r_{21}^i}{l_i}x - \frac{r_{22}^i}{l_i}y - \frac{r_{23}^i}{l_i}z)$$
$$+2k_2^i(\frac{r_{12}^i}{l_i})(H_{2i} + \frac{r_{11}^i}{l_i}x + \frac{r_{12}^i}{l_i}y + \frac{r_{13}^i}{l_i}z))$$

$$\frac{\partial E_p}{\partial z} = Mg + \frac{3m_l g}{2} + \sum_{i=1}^{3}(2k_1^i(-\frac{r_{23}^i}{l_i})(H_{1i} - \frac{r_{21}^i}{l_i}x - \frac{r_{22}^i}{l_i}y$$
$$-\frac{r_{23}^i}{l_i}z) + 2k_2^i(\frac{r_{13}^i}{l_i})(H_{2i} + \frac{r_{11}^i}{l_i}x + \frac{r_{12}^i}{l_i}y + \frac{r_{13}^i}{l_i}z)) \qquad (22)$$

The final forward dynamic equation of this parallel multi-body system can be written as:

$$\mathbf{M} \cdot \dot{\mathbf{u}} + \mathbf{K} \cdot \mathbf{q} = \mathbf{Q}_F + \mathbf{F}_D \qquad (23)$$

where $\mathbf{M} = (M + \frac{3}{4}m_l)\mathbf{I} + \frac{1}{3}m_l \sum_{i=1}^{3}\mathbf{M}_i$,

$$\mathbf{M}_i = \begin{bmatrix} (r_{21}^i)^2 + (r_{11}^i)^2 & r_{22}^i r_{21}^i + r_{12}^i r_{11}^i & r_{23}^i r_{21}^i + r_{13}^i r_{11}^i \\ r_{21}^i r_{22}^i + r_{11}^i r_{12}^i & (r_{22}^i)^2 + (r_{12}^i)^2 & r_{23}^i r_{22}^i + r_{13}^i r_{12}^i \\ r_{21}^i r_{23}^i + r_{11}^i r_{13}^i & r_{22}^i r_{23}^i + r_{12}^i r_{13}^i & (r_{23}^i)^2 + (r_{13}^i)^2 \end{bmatrix}$$

F_D is the disturbance force acting on the mass center of moving platform. $\mathbf{I}$ is the identity matrix. In this case, the pertinent flexure hinge stiffness has the relationship of

$$k_1^i = k_2^j = k \ (i = 1, 2, 3, j = 1, 2, 3)$$

Hence, the stiffness matrix of the whole system is:

$$\mathbf{K} = 2k \begin{bmatrix} \sum_{i=1}^{3}\frac{r_{21}^i{}^2 + r_{11}^i{}^2}{l_i^2} & \sum_{i=1}^{3}\frac{r_{21}^i r_{22}^i + r_{11}^i r_{12}^i}{l_i^2} & \sum_{i=1}^{3}\frac{r_{21}^i r_{23}^i + r_{11}^i r_{13}^i}{l_i^2} \\ \sum_{i=1}^{3}\frac{r_{21}^i r_{22}^i + r_{11}^i r_{12}^i}{l_i^2} & \sum_{i=1}^{3}\frac{r_{22}^i{}^2 + r_{12}^i{}^2}{l_i^2} & \sum_{i=1}^{3}\frac{r_{22}^i r_{23}^i + r_{12}^i r_{13}^i}{l_i^2} \\ \sum_{i=1}^{3}\frac{r_{21}^i r_{23}^i + r_{11}^i r_{13}^i}{l_i^2} & \sum_{i=1}^{3}\frac{r_{22}^i r_{23}^i + r_{12}^i r_{13}^i}{l_i^2} & \sum_{i=1}^{3}\frac{r_{23}^i{}^2 + r_{13}^i{}^2}{l_i^2} \end{bmatrix}$$

Let $\mathbf{F}^{a_i}$ be the vector of force exerted by the ith piezo actuator on each limb at the mass center of the strut in the global coordinate system. The generalized external force matrix is:

$$\mathbf{Q}_F = \sum_{i=1}^{3}\mathbf{F}^{a_i} + \begin{bmatrix} 2k\sum_{i=1}^{3}(\frac{r_{21}}{l_i}H_{1i} - \frac{r_{11}}{l_i}H_{2i}) \\ 2k\sum_{i=1}^{3}(\frac{r_{22}}{l_i}H_{1i} - \frac{r_{12}}{l_i}H_{2i}) \\ 2k\sum_{i=1}^{3}(\frac{r_{23}}{l_i}H_{1i} - \frac{r_{13}}{l_i}H_{2i}) - Mg - \frac{3m_l g}{2} \end{bmatrix}$$

Let the $\mathbf{F}_a$ be the matrix of scalars of driving forces given by:

$$\mathbf{F}_a = \begin{bmatrix} F_1 & F_2 & F_3 \end{bmatrix}^T \qquad (24)$$

where $\mathbf{F}^{a_i} = F_i \widehat{\mathbf{c}}_3^i$.

IV. Control Strategy

The simple form of loop shaping in scalar systems does not extend directly to multi-variable (MIMO) plants, which are characterized by transfer matrices instead of transfer functions. The notion of optimality is closely tied to MIMO control system design [6]. In this section, the control strategy will be analyzed by using the linear quadratic regulator (LQR) method, which is a well-known design technique that provides practical feedback gains.

A process of the active vibration control is shown in Fig. 3. The sensors on the moving platform detect the disturbances acting on the system first. Then the signals are converted by A/D signal converter and feed back to the controller to calculate the driving forces which will be sent to three piezo actuators, and finally realize the active vibration isolation. The block diagram for this feedback active vibration control is shown in Fig. 4, where $\underline{\varpi}$ is the

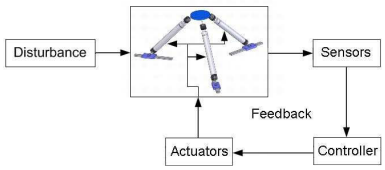

Fig. 3. Process of the active vibration control.

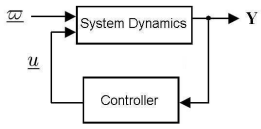

Fig. 4. Block diagram for feedback active vibration control.

disturbance vector, $\underline{u}$ is the control vector and $\mathbf{Y}$ is the measurement vector.

As shown in Fig. 5, let $\mathbf{X}_b$ and $\mathbf{X}_m$ be the 3 degree of freedom displacements of base platform and moving platform. Hence, the Eq. (23) can be written as:

$$\mathbf{M}\cdot\ddot{\mathbf{X}}_m+\mathbf{K}\cdot(\mathbf{X}_m-\mathbf{X}_b)=\mathbf{Q}_F+\mathbf{F}_D \tag{25}$$

According to the Eq. (25), the state vector consists of $\mathbf{X}_m$ with the 3 coordinates:

$$\begin{bmatrix}\dot{\mathbf{X}}_m\\ \ddot{\mathbf{X}}_m\end{bmatrix}=\begin{bmatrix}\mathbf{0} & \mathbf{I}\\ -\mathbf{M}^{-1}\mathbf{K} & \mathbf{0}\end{bmatrix}\begin{bmatrix}\mathbf{X}_m\\ \dot{\mathbf{X}}_m\end{bmatrix}+\begin{bmatrix}\mathbf{0} & \mathbf{0}\\ \mathbf{M}^{-1} & \mathbf{M}^{-1}\mathbf{K}\end{bmatrix}\cdot\begin{bmatrix}\mathbf{F}_D\\ \mathbf{X}_b\end{bmatrix}+\begin{bmatrix}\mathbf{0}\\ \mathbf{M}^{-1}\end{bmatrix}\mathbf{Q}_F \tag{26}$$

Let the state vector, disturbance vector and control vector be

$$\mathbf{X}=\begin{bmatrix}\dot{\mathbf{X}}_m\\ \ddot{\mathbf{X}}_m\end{bmatrix},\ \underline{\varpi}=\begin{bmatrix}\mathbf{F}_D\\ \mathbf{X}_b\end{bmatrix},\ \underline{u}=\mathbf{Q}_F$$

respectively. Hence, the generalized plant of the control problem is given by:

$$\dot{\mathbf{X}}=\mathbf{A}\cdot\mathbf{X}+\mathbf{B}\cdot\underline{u}+\mathbf{D}\cdot\underline{\varpi},\ \mathbf{Y}=\mathbf{X} \tag{27}$$

where

$$\mathbf{A}=\begin{bmatrix}\mathbf{0} & \mathbf{I}\\ -\mathbf{M}^{-1}\mathbf{K} & \mathbf{0}\end{bmatrix},\ \mathbf{B}=\begin{bmatrix}\mathbf{0}\\ \mathbf{M}^{-1}\end{bmatrix},$$

$$\mathbf{D}=\begin{bmatrix}\mathbf{0} & \mathbf{0}\\ \mathbf{M}^{-1} & \mathbf{M}^{-1}\mathbf{K}\end{bmatrix}.$$

Let the weighted matrix $\mathbf{Q}$ and $\mathbf{R}$ be:

$$\mathbf{Q}=\alpha\begin{bmatrix}\mathbf{K} & \mathbf{0}\\ \mathbf{0} & \mathbf{M}\end{bmatrix},\ \mathbf{R}=\beta\mathbf{I}. \tag{28}$$

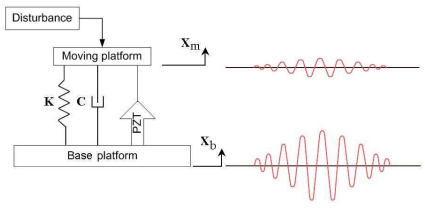

Fig. 5. Active vibration isolation system.

where α and β is the undetermined coefficient. The full state feedback controller gain matrix $\mathbf{G}$ can be solved by LQR method, and

$$\underline{u}=-\mathbf{G}\mathbf{X} \tag{29}$$

Substitute Eq. (29) to Eq. (27), the closed loop system dynamics is given by:

$$\dot{\mathbf{X}}=\widetilde{\mathbf{A}}\cdot\mathbf{X}+\mathbf{D}\cdot\underline{\varpi} \tag{30}$$

where $\widetilde{\mathbf{A}}=\mathbf{A}-\mathbf{B}\mathbf{G}$. Finally, the time response of the close loop control model can be obtained by using differential equation solver.

V. Numerical Simulations

The parameters of the parallel mechanism are shown in Table I. As the well elastic nature of the selected material of wide-range flexure hinges, the workspace of micro motion only depends on the limits of piezo actuator. The maximal usable inscribed workspace of micro motion, when the inputs of ceramic motors are zero and self-locked at the initial position, is a column with a radius of 66.6μm and 38.6μm height according to [5] of our previous work.

TABLE I

GEOMETRIC AND MATERIAL PARAMETERS

Item	Value
Radius of moving platform r	20mm
Radius of fixed platform R	60mm
Radius of flexure hinge r_f	0.9mm
Length of flexure hinge l_f	10mm
Radius of strut r_s	6.35mm
Length of strut l_s	120mm
Modulus of elasticity of flexure hinge E_f	130GPa
Modulus of elasticity of strut E_s	70GPa

A. Influence of Undetermined Coefficient

First, in order to determine the weighted matrix $\mathbf{Q}$ and $\mathbf{R}$, the influence of the undetermined coefficients α and β should be considered. Since the response and driving forces are related to the ratio of α and β, the value of β is set to 100 in this paper according to the empirical value. The trend of the z-axis response of moving platform and the maximal driving force is shown in Fig. 6. In this state, it is obviously that the maximal driving force can be decreased with increase the value of β. But the effect of control gets worse. In this case, in order to control the displacement of moving platform under $1nm$, α and β are set to 100 and 7×10^{-6} for taking consideration of the response of moving platform and maximal driving force.

B. Active Vibration Control

As shown in Fig. 7, the red lines represent to the open loop response of the moving platform and the blue lines represent to the close loop response by using LQR method. It is obviously that the disturbance could be eliminated about 50-70% especially the disturbance acting along the z-axis.

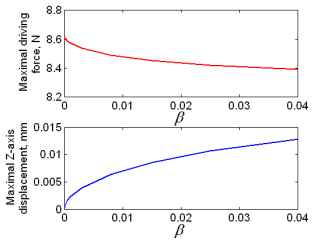

Fig. 6. Relationship between displacement/driving force and β (α=100).

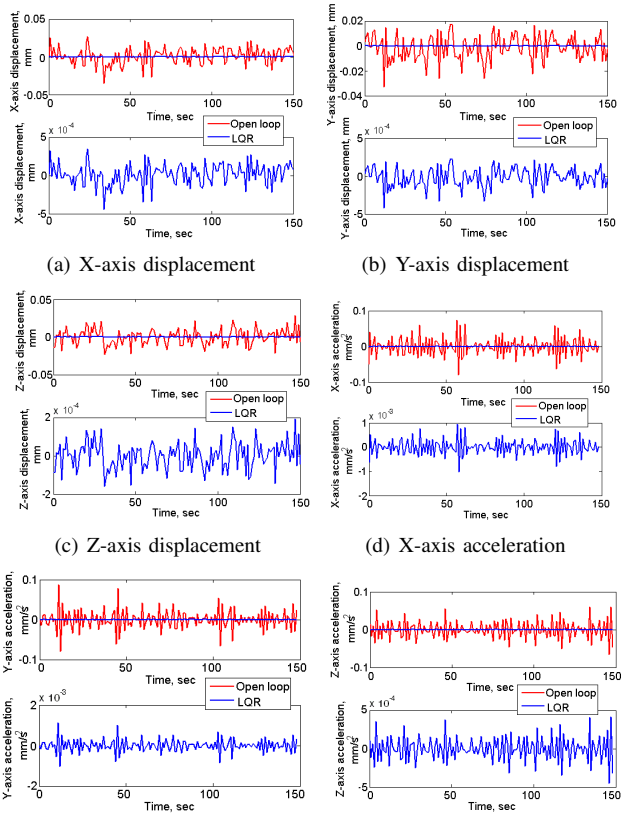

(a) X-axis displacement (b) Y-axis displacement

(c) Z-axis displacement (d) X-axis acceleration

(e) Y-axis acceleration (f) Z-axis acceleration

Fig. 7. Positions and accelerations of the moving platform

The change of the driving forces of three piezo actuators are shown in Fig. 8.

VI. Conclusion

In this paper, a novel dual 3-DOF parallel robot with flexure hinges has been presented. This system can achieve three high accurate translational positioning with a 3-DOF active vibration isolation and excitation function to the payload placed on the moving platform. Based on the previous research experiences in the systematical modeling and study of parallel robots, a vibrational model of the parallel manipulator has been presented by using Lagrange's dynamics. Then the active vibration control scheme for the MIMO system using LQR algorithm has been introduced. Finally, some simulation results by MATLAB are shown to verify the validity of the control strategy.

The investigations of this paper are expected to make

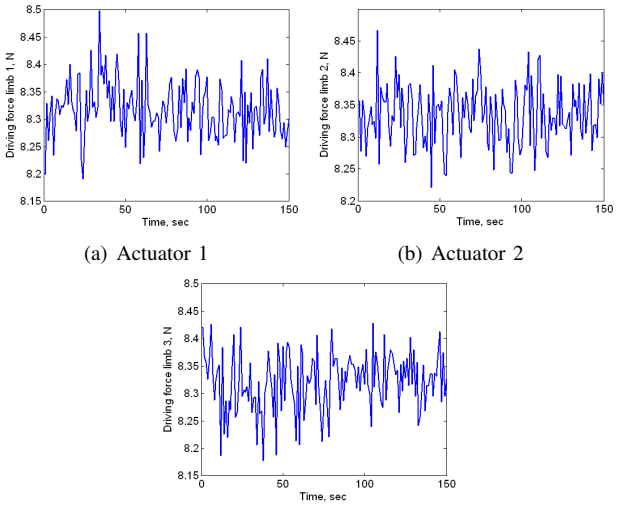

(a) Actuator 1 (b) Actuator 2

(c) Actuator 3

Fig. 8. Driving forces of the three actuators.

contributions to the research on active vibration isolation based on parallel manipulators. After this work, some control modeling for active vibration control will be given and optimal control algorithm will be discussed. Finally, a prototype of the parallel robot will be developed, and the experimental investigation will be carried out to verify the vibration control performance of the prototype.

References

[1] J. Hesselbach, A. Raatz, J. Wrege, and S.Soetebier, *Design and analysis of a macro parallel robot with flexure hinges for micro assembly tasks*, in Proc. of 35th International Symposium on Robotics, Paris, France, 2004, No.TU14-041fp.

[2] P. R. Ouyang, *Hybrid intelligent machine systems: Design, Modeling and Control*, Ph.D. Thesis, University of Saskatchewan, Canada, 2005.

[3] W. Dong, L. N. Sun, and Z. J. Du, *Design of a precision compliant parallel positioner driven by dual piezoelectric actuators*, Sensors and Actuators A: Physical, Vol. 135, pp. 250-256, 2007.

[4] X. Tang and I. -M. Chen, *A large-displacement 3-DOF flexure parallel mechanism with decoupled kinematics structure*, in IEEE/RSJ International Conference on Intelligent Robots and Systems, Beijing, China, 2006, pp. 1668-1673.

[5] Y. Yun and Y. Li, *Performance Analysis and Optimization of a Novel Large Displacement 3-DOF Parallel Manipulator*, in Proc. of IEEE International Conference on Robotics and Biomimetics, Bangkok, Thailand, pp.246-251.

[6] MIT, *Maneuvering and Control of Surface and Underwater Vehicles*, http://www.myoops.org/, Fall 2000.

[7] Y. Yun, Y. Li and Q. Xu, *Active vibration control on A 3-DOF parallel platform based on Kanes dynamic method*, in Proc. of SICE Annual Conference, Chofu, Tokyo, Japan, 2008, pp. 2783-2788.

[8] R. D. Hampton and G. S. Beech, *A Kane's Dynamics Model for the Active Rack Isolation System*, NASA/TMł2001C2110063, Marshall Space Flight Center, AL, 2001.

[9] Y. Li and Q. Xu, *Kinematic analysis and dynamic control of a 3-PUU parallel manipulator for cardiopulmonary resuscitation*, Proc. of 12th Int. Conf. on Advanced Robotics, pp. 344C351, 2005.

[10] M. S. Whorton, H. Buschek and A. J. Calise, *Homotopy Algorithm for Fixed Order Mixed H_2/H_∞ Design*, Journal of Guidance, Control, and Dynamics, Vol. 19, No. 6, pp. 1262C1269, 1996.

[11] M. Whorton, *Robust Control for Microgravity Vibration Isolation Using Fixed-order, Mixed H_2/μ Design*, AIAA Guidance, Navigation, and Control Conference and Exhibit, Austin, Texas, Aug. 11-14, 2003.